Drastic Photoemission Line Shape Changes in Li due to Surface-Bulk Interference and Plasmon Excitations

D. Claesson, S.-Å. Lindgren, and L. Walldén

Physics Department, Chalmers University of Technology, 41296 Göteborg, Sweden

T.-C. Chiang

Department of Physics, University of Illinois at Urbana-Champaign, 1110 West Green Street, Urbana, Illinois 61801-3080

(Received 2 July 1998)

Band mapping of Li by angle-resolved photoemission shows anomalous peak dispersion for near-uv photons, giving the false impression that an energy gap of about 1 eV is present just below the Fermi level. This is explained in terms of drastic line shape changes caused by interference between surface and bulk emission together with enhancements of these contributions for photon energies near the multipole surface plasmon and bulk plasmon energies, respectively. [S0031-9007(99)08468-9]

Angle-resolved photoemission is the most general tool for investigation of the occupied band structure of solids. Band mapping based on direct transitions has been successfully applied to numerous materials [1]. In the case of Li, a simple metal, one would expect the standard method to apply. We have taken a set of angle-resolved photoemission spectra in normal emission and expect to see a direct-transition peak dispersing continuously across the Fermi level in accordance with the known band structure [2] obtained from quantum well spectroscopy [3]. Instead, the spectra give the impression that a 1-eV-wide gap is present below the Fermi level, even though no such gap exists. This surprising observation has led us to reexamine the basic physics of photoemission.

Although it has been known for a long time that photoemission is due in part to the bulk and in part to the surface [4], the interference between these contributions and its influence on spectral line shapes has not been addressed until recently [5–7]. However, in these cases the line shape distortions are sufficiently mild that monitoring the direct-transition peak dispersion has not presented a problem. Is it then possible that surface emission is so strong in Li that the direct-transition peak becomes completely suppressed as a result of surface-bulk interference? A careful analysis of our data shows that this is indeed the case, and that it is due to the near-surface field associated with the multipole surface plasmon [8]. Evidence will be presented for this enhanced surface emission and a similar, albeit weaker, bulk plasmon resonance at higher energies. As the photon energy is scanned through the range used for band mapping, rapid intensity variations in surface and bulk emission as well as changes in their phase difference result in an apparent gap. The present study illustrates the complexity of the photoemission process and shows that coupling between the incident photon field and collective excitations may, together with interference, dominate the line shapes for simple metals.

The experiment was done at the MAX laboratory (Lund, Sweden) with synchrotron radiation in the 4.5 to 26 eV photon energy range. Photoelectron spectra were recorded in the normal emission direction from Li films with thicknesses up to 150 monolayers (ML) evaporated onto a Cu(111) crystal kept at a temperature of 120 K. Energy and angular resolutions were around 0.15 eV and 2°, respectively, while the light, incident at an angle of 45°, was *p* polarized. The low-energy electron diffraction (LEED) pattern was hexagonal indicating a (111)-oriented film with close packed planes, but we do not know whether the packing sequence is the 9*R* (Sm-type), characteristic of Li at low temperature [9]. The 150 ML film is thick enough to represent bulk Li. For thinner films, quantum well states are resolved, the energies of which can be used to determine the dispersion [2,3].

At high photon energies, the spectra exhibit a peak due to direct interband transitions in Li. This peak shifts from about 2 eV binding energy at $h\nu = 10$ to 1.2 eV binding energy at $h\nu = 6$ eV (Fig. 1). Above $h\nu = 10$ eV (not shown) the binding energy shifts towards the band bottom at 2.8 eV which is reached at $h\nu = 22$ eV. When the photon energy is decreased below 6 eV the interband peak stops shifting and its intensity diminishes rapidly, and, simultaneously, a peak emerges at the Fermi level. While the interband emission has a relatively modest intensity maximum at a photon energy close to 8 eV, the emission from the Fermi level has a strong maximum near $h\nu = 5.5$ eV. The inset in Fig. 1 (circles) shows a plot of binding energy versus photon energy for the two emission peaks seen in the spectra of Fig. 1. While this plot gives the impression that there is an approximately 1-eV-wide gap, no such gap exists. The spectra in Fig. 1 give no information about the dispersion for initial energies within 1.2 eV of E_F. The energies of quantum well states observed for thinner films show, however, that the dispersion is as expected for Li [10–12]. In the inset in Fig. 1 the solid curve shows the expected Li bulk peak dispersion. The dramatic difference between the band structure and the observed peak dispersion indicates that the usual method of band mapping by tracking the direct
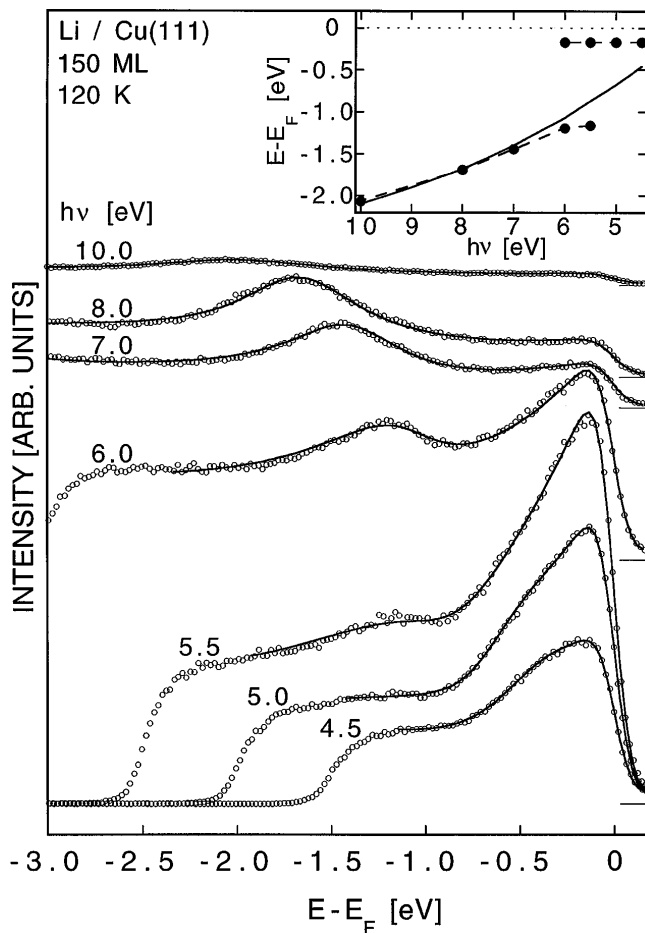
FIG. 1. Experimental photoemission spectra (circles) recorded in the normal emission direction from 150 ML of Li on Cu(111) at the indicated photon energies. The spectra are normalized to the incoming photon flux. Also shown are the corresponding calculated spectra (solid lines) obtained using the model described in the text. The inset shows initial state energy relative to the Fermi level versus photon energy for the two emission peaks seen in the experimental spectra (circles) and for direct interband transitions in Li according to the band structure used in the model calculation (solid curve). The dashed lines are guides to the eye.

interband transition as a function of photon energy in the near-uv range simply does not work in this case.

In order to understand the anomalous dispersion presented above, a calculation was performed in which the optical transition matrix element $M \propto \langle f | \mathbf{A} \cdot \nabla + \frac{1}{2} (\nabla \cdot \mathbf{A}) | i \rangle$ was combined with the initial and final densities of states according to Fermi's golden rule. The wave functions were obtained from a two-band model fit to the nearly-free-electron-like Li valence band (see the inset in Fig. 1). Individual effective masses were used for the initial and final bands. The initial state wave function was obtained by matching a linear combination of Bloch states within the crystal, one incident on the surface and one reflected, to an exponentially decaying tail on the vacuum side. Hole lifetime broadening was accounted for by

adding an imaginary term $\gamma/2$ with a quadratic binding energy dependence ($\gamma = \gamma_0 + aE_B^2$) to the initial state energy. According to the one step description of the photoemission process [13,14], the final state wave function is a time reversed LEED state. This state consists of a wave incident on the surface from vacuum together with one reflected and one transmitted component. The transmitted component was given an exponential envelope function having a decay length of 2λ where λ is the electronic mean free path. The Li-vacuum interface was modeled by a step potential at a distance z_0 beyond the classical surface. We used a value of z_0 near the one employed in Ref. [6] for Ag, which has a similar valence electron density. Instrumental broadening was accounted for by a Gaussian with a full width at half maximum of 0.15 eV, and the background of scattered electrons was modeled by the sum of two terms. One term, based on the "Shirley criterion" [15], represents scattering in the forward direction and the other term, having a quadratic binding energy dependence, represents isotropic scattering.

The $\mathbf{A} \cdot \nabla$ term in the matrix element is the usual bulk term responsible for direct interband transitions. The $\nabla \cdot \mathbf{A}$ term is usually taken to be zero with an appropriate choice of gauge. However, this assumption breaks down at a surface where the dielectric response changes abruptly. Furthermore, for photon energies in the range of collective electronic excitations, in particular, near the multipole surface plasmon mode, $\mathbf{A}$ has a rapid spatial variation near the surface which can give rise to a large $\nabla \cdot \mathbf{A}$ contribution [16]. The details have been worked out for jellium [17,18]. Here we adopt the semiclassical approximation and take $\nabla \cdot \mathbf{A}$ to be nonzero only at the surface. This allows us to rewrite the matrix element as

$$M \propto \sqrt{\frac{1-R}{h\nu}} \left[B(\nu) \int \psi_f^*(z) \frac{d\psi_i(z)}{dz} \, dz \right.$$
$$\left. + C(\nu) \psi_f^*(z_0) \psi_i(z_0) \right].$$

The factor in front of the bracket takes into account normalization to the photon flux and the reflectivity R of the surface. The first term within the bracket is the bulk term derived from $\mathbf{A} \cdot \nabla$, and the second term, derived from $\nabla \cdot \mathbf{A}$, is the surface term that involves the wave function amplitudes at the surface. The bulk and surface photoelectric coefficients B and C, generally complex, can have a significant frequency dependence due to plasmon excitations (see below).

The solid curves in Fig. 1 are fits to the data where the coefficients B and C are treated as adjustable parameters. These curves are seen to describe the data well. In particular, the gap and the peak intensity variations are well reproduced. In Fig. 2 are plotted, versus photon energy, the values of these parameters from the fit. Since the parameters are complex, the fit includes a determination of three quantities related to B and C, namely, their
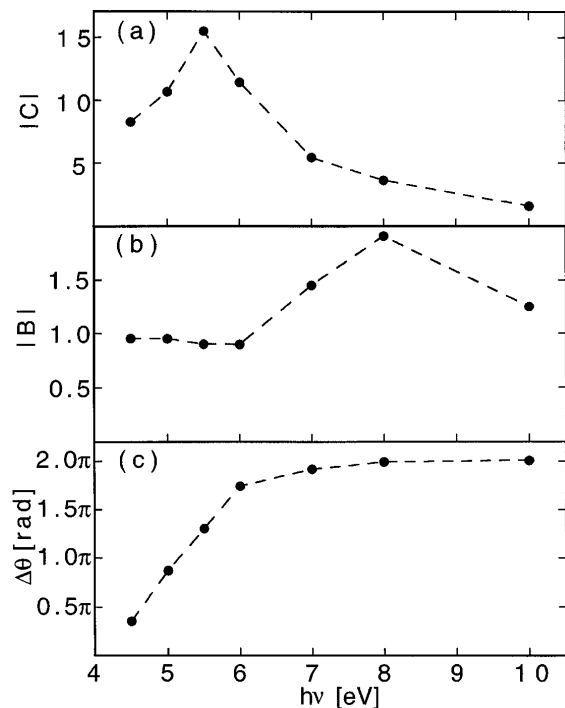
FIG. 2. Parameter values versus photon energy obtained from the fit of the model to experimental photoemission data (see Fig. 1). In (a) and (b) are plotted the amplitudes of the surface and bulk photoelectric constants, respectively, and in (c) the phase difference between them.

amplitudes [Figs. 2(a) and 2(b)] and their phase difference $\Delta\theta$ [Fig. 2(c)]. The amplitudes of B and C each show a maximum in the photon energy range probed. For C the peak is pronounced and located near 5.5 eV photon energy while for B the peak is weaker (relative to the background) and located near 8 eV. Other parameters used in the fit include the constants $\gamma_0 = 0.2$ eV and $a = 0.05$ eV^{-1} in the hole lifetime formula and the final state mean free path $\lambda = 5$ Å.

The appearance of a large emission peak at the Fermi level near $h\nu = 5.5$ eV (see Fig. 1) is caused by the strong enhancement of the surface photoelectric coefficient C [see Fig. 2(a)]. This energy corresponds well to the surface multipole plasmon resonance in Li. According to self-consistent jellium calculations [17] the photon field has a strong spatial variation close to the surface for energies near $0.8\hbar\omega_p$ (ω_p is the bulk plasma frequency) resulting in a large surface emission (due to $\nabla \cdot \mathbf{A}$) [16,18]. This surface response is associated with the excitation of a multipole surface plasmon mode [8] for which the induced charge has dipolar character normal to the surface in contrast to the monopole character of the ordinary surface plasmon. Given $\hbar\omega_p \approx 7$ eV for Li [19,20], the multipole surface plasmon mode should be near 5.5 eV, in agreement with the peak position of C as observed in the present experiment. The width of this multipole surface plasmon resonance as seen in Fig. 2(a) is also in

rough agreement with the width obtained from a photo-yield measurement for 38 ML Li on Al(111) [21].

As mentioned above, the interband peak seen in Fig. 1 has a maximum intensity near 8 eV. This is caused by an enhanced bulk photoelectric coefficient B, as seen in Fig. 2(b), which corresponds to excitation of the bulk plasmon mode. The presence of a surface allows the excitation of a longitudinal electric field associated with bulk plasmons [22]. This excitation has a threshold at ω_p [23] and reaches a maximum at a slightly higher frequency [17]. The enhanced field strength will lead to an enhanced bulk emission, which is observed as a peak in B near 8 eV photon energy. Further support for this interpretation is given by a related observation in spectra for 100 ML of K on Cu(111) of a pronounced maximum in the K valence band emission at 4 eV photon energy [24] which, as in the case of Li, is just above the bulk plasmon energy. In addition, recent photoyield measurements probing initial states just below the Fermi level have revealed that the excitation of overlayer bulk plasmons in alkali overlayers may induce electron emission [21].

The rapid change in relative strength of the surface and bulk contributions to the photoemission signal cannot by itself explain the drastic line shape change observed. Interference between emission from the surface and the bulk is also an important factor. This is evident from Fig. 3 where the calculated spectrum (solid curve) for $h\nu = 6.0$ eV is compared with a corresponding curve for which the bulk emission has been omitted ($B = 0$) (dotted curve) and thus only surface emission contributes. Likewise, the dash-dotted line represents emission from the bulk alone (magnified by a factor of 9). It is clear that the surface emission is the dominating contribution to the spectrum because the photon energy is near the peak of the multipole surface plasmon resonance. More interesting is the influence of interference between surface and bulk emission on the line shape. For binding energies above 1 eV the total emission is higher than the surface emission, indicating constructive surface-bulk interference, while for binding energies below 1 eV the total emission is lower than the surface emission, indicating destructive interference. The change from constructive to destructive interference at $\sim$1 eV is evident from the inset in Fig. 3 where the phase difference $\Delta\varphi$ between the bulk and surface contributions to the matrix element is plotted versus binding energy. The fact that a larger part of the bulk peak is located within the range of destructive interference and a smaller part, on the low energy side, is located outside this range, results in a pronounced minimum in the total emission, shifted slightly upwards in energy relative to the bulk peak, and a relatively weak maximum in the total emission shifted downwards. As the photon energy is decreased, the bulk peak energy and the range for destructive interference move towards each other and between 5.5 and 5.0 eV photon energy they coincide, resulting in an effective suppression of the bulk peak. For
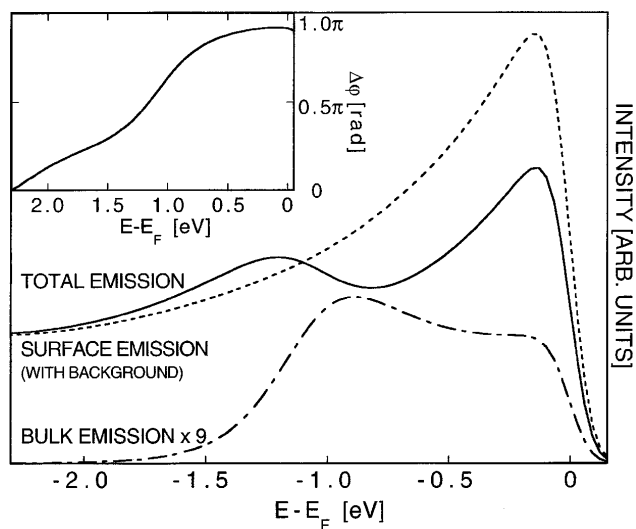
FIG. 3. Calculated photoemission spectrum for $h\nu = 6$ eV (solid line) together with the calculated contributions to the emission from the surface (dotted line) and from the bulk (dash-dotted line). Background emission is included in the surface contribution but omitted in the bulk contribution. The inset shows the phase difference between the bulk and surface contributions to the transition matrix element plotted versus initial state energy.

even lower $h\nu$ the bulk peak shifts further upward in energy and contributes to the emission peak near the Fermi level. This analysis thus shows that surface-bulk interference may cause a total suppression of the bulk peak near the multipole surface plasmon resonance.

In conclusion, photoemission band mapping of Li shows anomalous peak dispersion for photon energies below 7 eV, giving the false impression that a 1-eV-wide energy gap is present just below the Fermi level. The line shapes are reproduced in a model calculation and explained in terms of photoelectron interference between surface and bulk emission in combination with a rapid change in relative strength of these two contributions as the photon energy is varied. The change in relative strength is due to variations of the induced photon field in the vicinity of the surface caused by the excitation of surface and volume plasmon modes. This work illustrates that simple metals can exhibit complex line shapes associated with collective bulk and surface excitations and their interference. While the present work provides a qualitative understanding of the mechanism behind the photoemission line shape, a rigorous many-body calculation is called for in order to account for the electronic response in more detail. We finally point out that the effect discussed here should, with varying importance, be general for solid materials.

[1] See, for example, S. Hüfner, *Photoelectron Spectroscopy* (Springer, Berlin, 1995), 2nd ed.

[2] D. Claesson, S.-Å. Lindgren, and L. Walldén (to be published).

[3] For the procedure, see S.-Å. Lindgren and L. Walldén, Phys. Rev. Lett. **61**, 2894 (1988); M. A. Mueller, T. Miller, and T.-C. Chiang, Phys. Rev. B **41**, 5214 (1990).

[4] See, for example, *Angle-Resolved Photoemission,* edited by S. D. Kevan, Studies in Surface Science and Catalysis Vol. 74 (Elsevier, Amsterdam, 1992).

[5] K. W.-K. Shung and G. D. Mahan, Phys. Rev. Lett. **57**, 1076 (1986).

[6] T. Miller, W. E. McMahon, and T.-C. Chiang, Phys. Rev. Lett. **77**, 1167 (1996).

[7] E. D. Hansen, T. Miller, and T.-C. Chiang, Phys. Rev. Lett. **78**, 2807 (1997).

[8] See K.-D. Tsuei, E. W. Plummer, A. Liebsch, K. Kempa, and P. Bakshi, Phys. Rev. Lett. **64**, 44 (1990), and references therein.

[9] H. G. Smith, Phys. Rev. Lett. **58**, 1228 (1987).

[10] W. Y. Ching and J. Callaway, Phys. Rev. B **9**, 5115 (1974).

[11] J. C. Boettger and S. B. Trickey, Phys. Rev. B **32**, 3391 (1985).

[12] M. Sigalas, N. C. Bacalis, D. A. Papaconstantopoulos, M. J. Mehl, and A. C. Switendick, Phys. Rev. B **42**, 11 637 (1990).

[13] I. Adawi, Phys. Rev. **134**, A788 (1964).

[14] G. D. Mahan, Phys. Rev. B **2**, 4334 (1970).

[15] D. A. Shirley, Phys. Rev. B **5**, 4709 (1972).

[16] H. J. Levinson, E. W. Plummer, and P. J. Feibelman, Phys. Rev. Lett. **43**, 952 (1979).

[17] P. J. Feibelman, Phys. Rev. B **12**, 1319 (1975).

[18] P. J. Feibelman, Phys. Rev. Lett. **34**, 1092 (1975).

[19] T. A. Callcott and E. T. Arakawa, J. Opt. Soc. Am. **64**, 839 (1974).

[20] P. C. Gibbons, S. E. Schnatterly, J. J. Ritsko, and J. R. Fields, Phys. Rev. B **13**, 2451 (1976).

[21] S. R. Barman, K. Horn, P. Häberle, H. Ishida, and A. Liebsch, Phys. Rev. B **57**, 6662 (1998).

[22] See, for example, A. Zangwill, *Physics at Surfaces* (Cambridge University Press, Cambridge, England, 1988).

[23] A. R. Melnyk and M. J. Harrison, Phys. Rev. B **2**, 835 (1970); **2**, 851 (1970).

[24] D. Claesson, S.-Å. Lindgren, and L. Walldén (to be published).